Indian Journal of Natural Products and Resources
Vol. 17(1), March 2026, pp. 80-95
DOI: 10.56042/ijnpr.v17i1.20698

Antiproliferative and cytotoxic effects of *Boerhaavia diffusa*-derived sitosteryl oleate and its derivatives in human glioblastoma (U-87) cells

Rakhi Srivastava[1], Nalini Yadav[1], Lucky[1], Daman Saluja[1] and Madhu Chopra[1,2]*

[1]Dr. B. R. Ambedkar Center for Biomedical Research, University of Delhi, Delhi 110007, India

[2]Delhi School of Public Health, Institution of Eminence, University of Delhi, Delhi 1100007, India

Received 16 June 2025; revised received 27 February 2026; accepted 11 March 2026

Phytosterols present in free form and in esterified form with fatty acids, sugar moieties, or phenolic acids show antiproliferative properties on several cancers. This study reports the isolation, characterisation, and evaluation of the bioactive anticancer ester, sitosterol oleate (BDPT-3), from *Boerhaavia diffusa*, which induced significant cell death in U-87 MG cells with an IC_{50} of 184 µM. A cell viability assay showed that it significantly inhibited U-87 cell proliferation. Morphological changes, DNA fragmentation, AO/EB staining, and cell cycle analyses in U-87 cells confirmed that it induced apoptosis. It altered the Bax/Bcl-2 ratio by decreasing BCL-2 expression while Bax expression was relatively constant. Further, sitosteryl oleate and its analogues were synthesised, characterised, and evaluated for antiproliferative activity. Among them, butanoate (2c), pentanoate (2d), and decanoate (2h) derivatives showed IC50 values between 60 and 70 µM, and benzoate (2j) showed an IC50 value of 91.77 µM after 72h. Further *in vitro* and *in vivo* studies are needed to validate their therapeutic potential against glioblastoma.

Keywords: Apoptosis, *Boerhaavia diffusa*, Cytotoxic, Glioblastoma, Phytosterols, Sitosteryl oleate

IPC code; Int. cl. (2021.01)− A61K 36/00, A61P

Introduction

Analysis of the health-endearing properties of fruits and spices has led to the identification and isolation of a vast cluster of bioactive compounds in plants, such as phytosterols, coumarins, phenolics, limonoids, flavonoids, and carotenoids, etc.[1–3]. Consuming fruits and vegetables is essential for maintaining a healthy lifestyle and protecting against several diseases, such as chronic heart disease[4], cancer[5], Parkinson's disease[6], Alzheimer's disease[7], diabetes[8], and viral infections[9]. Several epidemiological studies have shown that regular intake of fruits and vegetables has an inhibitory effect on the development of cancer[10,11]. Phytochemicals are mainly responsible for this inhibitory action. Chemoprevention of tumorigenesis is one of the major measures used to decrease the number of cancer cases. Dietary ingredients and phytochemicals are the major repertoires for identifying chemopreventive chemicals against tumorigenesis[12].

Boerhaavia diffusa (Punarnava) roots have been mentioned in Ayurveda for various ailments such as Sopha (Fever), Pandu (Anemia), Hridroga (heart-related problems), Kasa (Cough), Arsa (piles), Urahksatasa (lung disease), and sotha (oedema)[13,14]. *B. diffusa* roots have been extensively used and feature a wide range of biological activities such as anticancer, anthelmintic, antioxidant, and neuropharmacological effects[15]. A scientific analysis of the medicinal properties of Punarnava root has exposed its antiproliferative, immunomodulatory, anti-inflammatory, anti-convulsant, and hepatoprotective activities[16]. In a study conducted by Manu *et al*., it was found that punarnavine, an alkaloid isolated from Punarnava's root, could inhibit the metastatic progression of B16F-10 melanoma cells in mice[17,18]. Previous work from our lab showed that a purified fraction from the ethanolic root extract of *B. diffusa* showed S-phase inhibition and apoptosis in HeLa cells[19]. Several compounds such as boeravinones, β-sitosterol, β-sitosterol-β-D-glucoside, tetracosanoic, hexacosanoic, stearic, palmitic, arachidic acids, hextriacantane, and urosolic acid have been isolated and identified from Punarnava root[20].

*Correspondent author
Email: mchopradu16@gmail.com, mchopra@acbr.du.ac.in
Supplementary tables and figures are available online only.

Phytosterols are abundant in fruits, vegetables, and nuts. Among the plant sterols, sitosterol, campesterol, and stigmasterol are the chief plant sterols, which are structural analogues of cholesterol. Phytosterols occur in nature in the free form as well as in esterified form with fatty acids, sugar moieties, or phenolic acids. Several studies have shown the potential of plant sterols to lower cholesterol *levels in vivo* by reducing their uptake via the LDL receptor[21,22] and by lowering their absorption in the small intestine[23,24]. Thus, they also prevent coronary heart disease and cardiovascular risks[25–27]. Several studies showed antiproliferative properties of plant sterols along with β-sitosterol on human breast cancer[28], Cervical cancer[19,29], and colon cancer HCT116 cells[30], lung cancer[31], digestive cancer[32], colorectal cancer[33], liver cancer[34], pancreatic cancer[35], leukemia and multiple myeloma[36], ovarian cancer[37], prostate cancer cells[38]. It has been suggested that antiproliferative effects shown by β-sitosterol are related to the activation of the sphingomyelin cycle and/or to cell cycle arrest[39]. An increase in the level of the proapoptotic protein Bax and induction of caspases may be the possible mechanism behind the apoptotic cell death induced by β-sitosterol[40,41].

Apoptosis is a genetically programmed cell death that is an essential process for the normal development and maintenance of tissue homeostasis. It also leads to the elimination of unwanted or damaged cells from multicellular organisms[42]. In many diseases, such as cancer, autoimmune diseases, and neuronal conditions, cells evade the process of apoptosis[43]. Therefore, understanding the mechanisms of apoptosis is essential for preventing and treating many diseases. The characteristics of apoptotic cells include distinct morphological changes, such as cell shrinkage, mitochondrial depolarisation, plasma membrane blebbing, chromatin condensation, and DNA fragmentation. The induction of apoptosis in tumour cells is the most common anticancer mechanism targeted by many cancer therapies. Therefore, there is a need to identify potential therapeutic anti-tumour drugs with potent and selective apoptotic effects. The present study focuses on Glioblastoma. Glioblastoma, an intrinsic brain tumour that can progress at any age, is caused by genetic alterations that impact neuroglial stem or progenitor cells. As people age, the incidence rises continuously[44]. One of the most aggressive and deadly cancers is glioblastoma, which accounts for 80% of all malignant brain tumours and 30% of primary ones[45]. Less than 5% of patients with glioblastoma survive five years after diagnosis, with a median overall survival of 14.6 to 20.5 months[46]. Glioblastoma is often treated with surgical excision, radiation therapy, and chemotherapy using the drug temozolomide (TMZ). It continues to have one of the lowest survival rates among all cancer types, even with varying treatment modalities. To date, no known causes of glioblastoma have been identified. Furthermore, the blood-brain barrier (BBB) reduces the effectiveness of chemotherapy by preventing drugs from reaching the central nervous system. Additionally, the onset of multidrug resistance may further decrease the effectiveness of chemotherapy medications[47]. The discovery of novel, targeted, and efficient medicines is therefore critically needed to treat glioblastoma.

For many years, people have been interested in using natural products to prevent sickness, promote physical and mental health, and maintain a healthy state. Several studies have documented the radio/chemoprotective function of several natural substances in conjunction with chemotherapy and radiation therapy, as well as their synergistic effects in reducing side effects and boosting the effectiveness of cancer treatments[48]. In the present study, a bioactivity-guided isolation was performed from the ether extract of *B. diffusa* plant. The structure of the isolated compound was established as sitosteryl oleate using spectroscopic techniques. The isolated active compound, sitosteryl oleate, was further evaluated for its biological activities in glioblastoma cells (U-87 MG) by investigating the effects on cell proliferation and apoptosis induction. Further, to increase the pharmacokinetic properties of the lead compound, sitosteyl oleate, we synthesised a series of ten ester analogues of β-sitosterol and evaluated their antiproliferative activity in glioblastoma cells (U-87 MG).

Materials and Methods

Plant sample collection, identification, and extraction

Plant material and extraction procedures, *B. diffusa* was collected during the month of April/May in 2011, from Gwalior (Madhya Pradesh), India. The identification of the herb was done by Dr Gurcharan Singh, Taxonomist, Dept. of Botany, Sri Guru Teg Bahadur Khalsa College, University of Delhi, Delhi. The dried roots of this plant were ground into powder

after being cut into small pieces. The powder (400 g) was macerated with ether (1 L) and allowed to stand for about 24 h at room temperature, and the procedure was repeated six times. The above ether solutions were combined and concentrated to yield a white precipitate, and the flask was kept at 4ºC overnight to get proper precipitation. The precipitate was collected by filtration (40 mg), and the concentrated ether solution freed from the precipitate was evaporated to dryness. The resultant yellow-brown residue (3.3 g) was dissolved in ether (200 mL) and extracted with saturated aqueous Na_2CO_3. The aqueous layer was then back-extracted with ether. The aqueous layer was made slightly acidic (pH 6) by adding 10% HCl, and the mixture was then extracted with ether. The combined ether layers were evaporated to yield an acidic substance as oil (150 mg).

The remaining ether solution from the Na_2CO_3 treatment was washed with saturated NaCl, dried over anhydrous sodium sulphate, and evaporated to give a greasy residue (3 g), named as crude ether extract.

Bioactivity-guided purification of *B. diffusa* ether crude ether extract

The crude ether extract was purified by column chromatography (silica gel, mesh size 60-200 mm). The mobile phase consisted of combinations of petroleum ether, chloroform, and Methanol (MeOH), and the polarity of the mobile phase was gradually increased by increasing the composition of the more polar solvent (methanol). The eluent was collected in fractions of 300 mL each. The chemical composition of each fraction was evaluated by thin-layer chromatography (TLC) and visualised under UV (254 and 365 nm) and iodine vapour. Based on the TLC profiles, fractions with similar compositions were pooled together and concentrated under reduced pressure. Based on TLC, we selected 4 major fractions for cytotoxicity testing.

All four fractions obtained through column chromatography were subjected to an antiproliferation assay on HeLa cells, and fraction 3 ($CHCl_3$: MeOH - 97:3) was the most active. TLC profile of fraction 3 (ETR 3; 30 mg) showed one major spot, which was further purified by preparative TLC on silica gel using $CHCl_3$–MeOH (97:3) as the solvent, yielding sitosteryl oleate (BDPT-3) (20 mg). The HPLC of sitosteryl oleate (BDPT-3) was performed with a Shimadzu HPLC system using a reverse-phase C-18 column and a UV detector (222 nm). Methanol: water 50:50; v/v was used as the mobile phase, and the flow rate was maintained at 1 mL/min. The detailed process of purification of the ether extract is summarised in Fig. 1. Sitosteryl oleate (BDPT-3) showed a single peak in the HPLC chromatogram (Fig. 2). This compound BDPT-3 was characterised as sitosteryl oleate (Fig. 3) with the help of spectroscopic techniques using IR, NMR, and MASS and comparison with earlier reported structure. The structure was also confirmed by the synthesis of the compound and by spectral comparisons. (Supplementary Table 1).

Maintenance of the cell line and preparation of the sample for cytotoxicity evaluation

U-87 MG (human glioblastoma) cells were purchased from NCCS, Pune, and cultured in Dulbecco's Modified Eagle Medium (Sigma, St. Louis, USA) supplemented with 10% heat-inactivated Foetal Bovine Serum (GIBCO) and 1% Penicillin-streptomycin (Sigma, St. Louis, USA). The cells were incubated in a humidified atmosphere of 5% CO_2 at

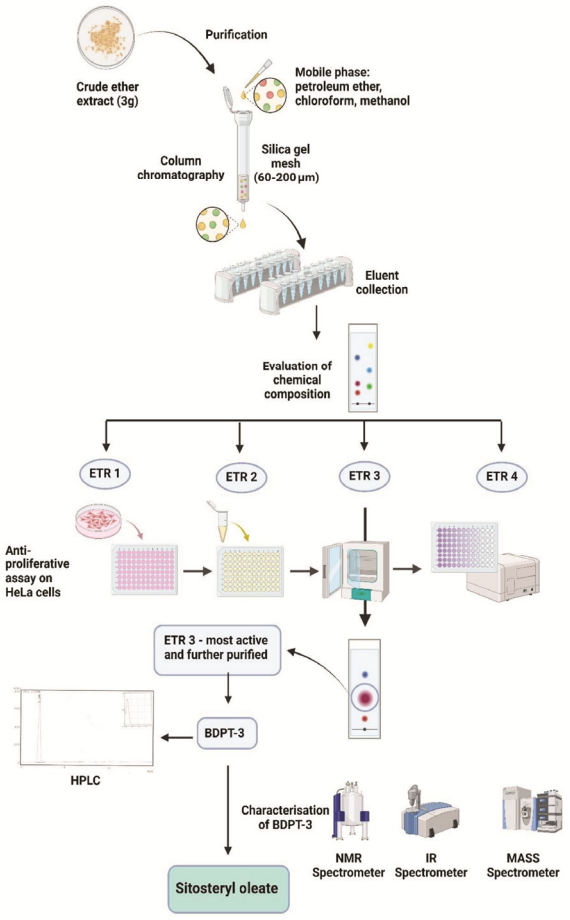

Fig. 1 — Bioactivity-guided purification and fractionation on silica gel column chromatography of the ether root extract.

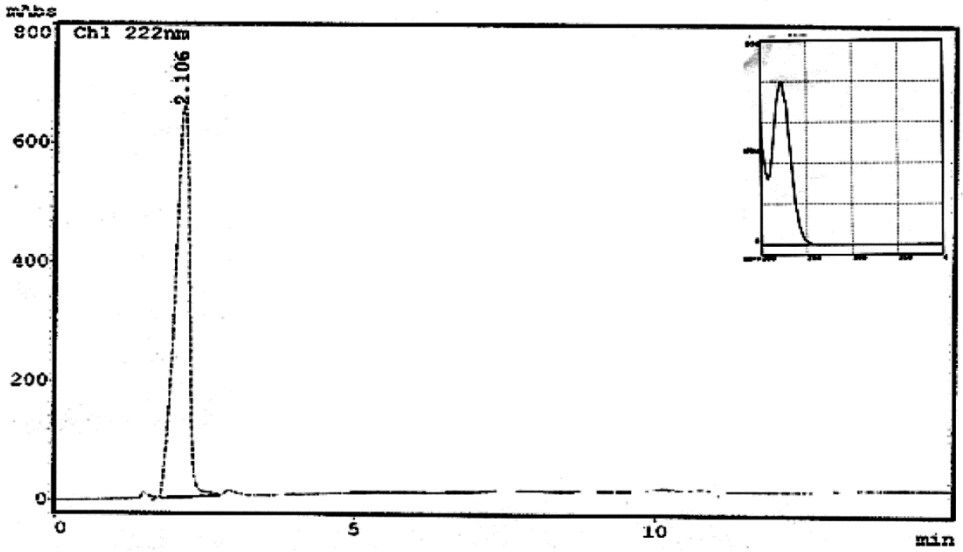

Fig. 2 — HPLC profile of purified compound from ether extract (BDPT-3). Chromatogram of active sitosteryl oleate (BDPT-3) isolated from BD ether extract fraction 3 (ETR 3) resolved using mobile phase methanol: water (50:50) v/v at a flow rate of 1 mL/min.

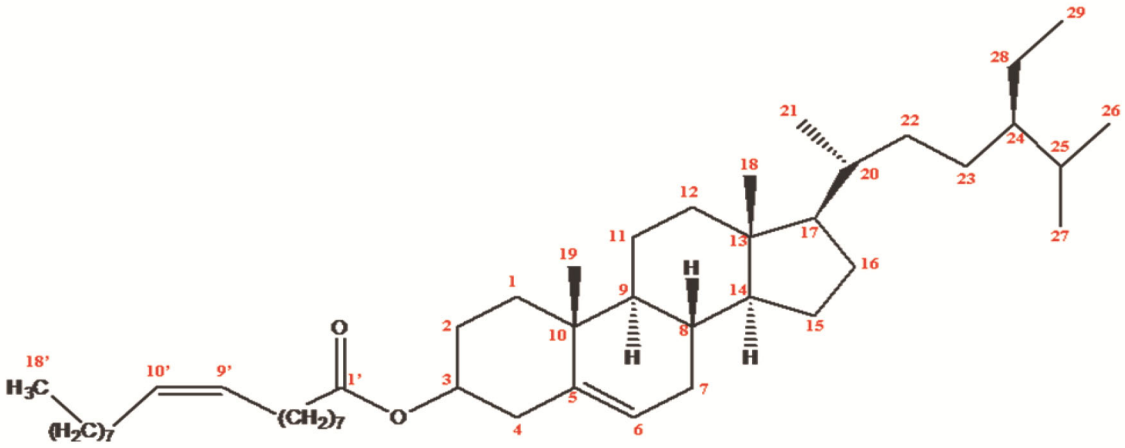

Fig. 3 — Structure of sitosteryl oleate.

37ºC. Sitosteryl oleate (BDPT-3), isolated and purified from *B. diffusa,* was dissolved in PEG:EtOH (2:3) and diluted into culture medium. The PEG: EtOH concentration used to dissolve the extract was not cytotoxic to the same cell line.

***In vitro* cytotoxicity assay**

Cell survival was measured using the MTT microculture tetrazolium assay, as described by Mosmann (1983). A total of 1000 cells/well were seeded in a 96-well plate. After 24 h incubation in a 5% humidified CO_2 incubator at 37ºC, varying concentrations of sitosteryl oleate (BDPT-3) were added to a final volume of 200 µL of standard growth medium/well. The concentration of PEG: EtOH used to dissolve the extract did not exceed 0.75% (v/v). Therefore, the same PEG: EtOH concentration was used in the control wells. Methotrexate (at a concentration of 10, 20, 50, 100, and 200 nM) was used as a positive control. After 24 h incubation at 37ºC, 20 µL of MTT [3-(4,5-dimethylthiazol-2-yl)-2,5-diphenyltetrazolium bromide] (Invitrogen) (5 mg/mL in PBS) was added to each well and incubated for 4 h at 37ºC. The medium was removed, and formazan crystals thus formed were dissolved in DMSO. The plates were read immediately in a microplate reader (Tecan, Genios-Pro, Austria) operating at 540 nm.

Trypan blue dye exclusion assay for viability

The effect of sitosteryl oleate (BDPT-3) on cell viability was assessed using a trypan blue dye-

exclusion test under a light microscope (Nikon, Japan). 0.15×10^6 cells were plated in 40 mm dishes. 24 h after plating, cultures were treated with vehicle [(PEG: EtOH (2:3)] alone or sitosteryl oleate (BDPT-3) at different concentrations and incubated further for 24 h. After incubation, treated cells were trypsinised and counted in a hemocytometer using 0.4% trypan blue (HiMedia). Dead cells retained the dye while the viable cells excluded trypan blue and appeared bright. Cell death at different treatment time points was calculated as follows:

% Cell death = [number of dead cells/ (number of viable cells + number of non-viable cells)] ×100.

Morphological analysis

U-87 cells in the exponential growth phase were plated at 2×10^4 cells in a 40 mm petri plate. After 24 h of growth, cells were treated with sitosteryl oleate (BDPT-3) (50, 100 µg/mL) and vehicle control, respectively, for 24 h. At the end of the treatment period, the effect of sitosteryl oleate (BDPT-3) on the morphological change of the U-87 cells was assessed by the inverted and phase-contrast microscope (Nikon, Japan) at 100 X magnification.

AO/EB staining for apoptotic cells

Acridine orange is taken up by both viable and non-viable cells. It emits green fluorescence if intercalated into double-stranded nucleic acid (DNA) or red fluorescence if bound to single-stranded nucleic acid (RNA). Ethidium bromide is taken up only by non-viable cells and emits red fluorescence by intercalation into DNA. We distinguished three cell types based on fluorescence emission and the morphological features of chromatin condensation in the stained nuclei. Viable cells have uniform, bright-green nuclei with an organised structure. Apoptotic cells have orange to red nuclei with condensed or fragmented chromatin. Necrotic cells have uniformly orange to red nuclei with an organised structure. 10 µL of dye mixture (100 µg/mL AO and 100 µg/mL EB in distilled water) was mixed with 10 µL of cell suspension (0.1×10^6 cells/mL) on a clean microscope slide. The suspension was immediately examined by fluorescence microscopy (Nikon, Japan) at 100 X magnification. A minimum of 300 cells was counted in every sample.

Analysis of DNA fragmentation

U-87 cells (0.5×10^6) were incubated for 24 h in a medium containing 10% FBS. After 24 h, cells were treated with sitosteryl oleate (BDPT-3) at concentrations of 50, 100, and 200 µg/mL, and with the vehicle control. Methotrexate at 100 nM was used as a positive control. Thereafter, cells were collected by trypsinisation and rinsed twice in cold phosphate-buffered saline (PBS, pH 7.4). Genomic DNA was extracted from U-87MG cells using the centrifuge protocol of the AxyPrep Multisource Genomic DNA Miniprep Kit. Isolated DNA was analysed by agarose gel electrophoresis.

Cell cycle analysis

Flow cytometry was used to detect the apoptotic rate quantitatively. Flow cytometric DNA analyses estimated the distribution of cells across different stages of the cell cycle. Briefly, 2×10^5 cells were incubated overnight in 60 mm culture dishes in a medium containing 10% FBS. After 24 h, cells were treated with sitosteryl oleate (BDPT-3) at different concentrations. Cells were harvested after 24 h, washed twice with cold PBS (pH 7.4), and fixed with 70% ethanol/ 30% PBS at 4ºC. Flow cytometric measurements of cellular DNA content were performed with the ethanol (70%) fixed cells using the intercalating DNA fluorochrome, Propidium Iodide (PI, Sigma, St. Louis, MO, USA). The fixed cells were washed with PBS to remove ethanol and incubated with 0.2 mL PBS containing RNase (200 µg/mL) (Sigma, St. Louis, USA) and incubated at 37ºC for 30 minutes, then stained with 50 µg/mL propidium iodide for 30 minutes in the dark at room temperature, and finally analysed on a FACS cytometer (Calibur™, Becton Dickinson, USA). A minimum of 1×10^4 cells/sample was evaluated, and the percentage of cells in each cell cycle phase was calculated using the CELLQUEST and Modfit software (Becton Dickinson).

Western Blot Analysis

Following appropriate treatment, cells were detached from the substrate and collected by centrifugation (600 g, 5 min, 4ºC). The pellets were washed with 1 mL of ice-cold PBS and collected again via centrifugation (600 g, 5 min, 4ºC) and resuspended in lysis buffer containing 25 mM HEPES, 5 mM $MgCl_2$, 2 mM EDTA, 2 mM DTT, 1 mM PMSF, 1 mM sodium orthovanadate, and 1% protease inhibitor cocktail (Sigma). The lysis buffer for whole-cell lysates also contained 1% SDS and 1% Triton X-100. Lysates of 5×10^6 cells were sonicated and then centrifuged (10 000 r.p.m., 10 min, 4ºC).

After sonication, lysates were centrifuged as detailed above, and the supernatant was collected.

Equal amounts of protein (50 µg), as determined using the Bradford Protein estimation kit (GeNei^{TM}, Bangalore GeNei, India), were loaded and resolved using 12% SDS-PAGE and transferred onto PVDF membranes (MDI, Ambala, India). Blots were blocked overnight at 4ºC in PBS – Tween 20 (0.05%) - BSA (3%) and then incubated with primary antibody in blocking buffer (overnight, 4ºC). Anti bcl-2 (SC-7382), anti-bax (SC-7480), anti p53 (SC-98), and anti β-actin (SC-1615) were the primary antibodies used in this study. Goat anti-mouse IgG-HRP (SC-2005) and donkey anti-goat IgG-HRP (SC-2020) were secondary antibodies. All the antibodies were purchased from Santa Cruz Biotechnology (Santa Cruz, CA, USA). After washing with PBS containing 0.05% Tween (PBS-T), blots were incubated with the secondary antibody for 2 h at 4ºC. After successive washes, the signal was detected by chemiluminescence (SuperSignal, Pierce, USA). We used Syngene Chemiluminescent imaging systems (Syngene, Cambridge, UK) to exclusively capture chemiluminescent blots. The blot was developed on GeneSnap acquisition software after an appropriate exposure time. GeneTools analysis software was used to quantify the bands.

Statistical analysis

The experiments were performed in triplicate, and all experimental data are expressed as mean±SD. The statistical significance of the difference between control and BD extract-treated groups was determined by one-way ANOVA followed by Dunnett's t-test for multiple comparisons and by Student's t-test. The result was considered significant at $P < 0.05$.

Chemicals and reagents for synthesis of β-sitosterol ester analogues

All chemicals and reagents were of analytical grade and purchased from TCI, Sigma-Aldrich, Spectrochem, and SD Fine Chemicals Pvt. Ltd., India, and used without further purification. The chemical reactions were monitored by TLC on commercially available silica gel 60 F254-coated alumina plates (Merck). TLC, ^{1}H NMR, ^{13}C NMR, and Mass spectroscopy confirmed the purity of all organic compounds. ^{1}H NMR and ^{13}C NMR spectra were recorded in Jeol instrument (model-JNM-EXCP 400) operating at 400 MHz (^{1}H) in $CDCl_3$ and at 100 MHz (^{13}C) using TMS as an internal standard. The chemical shifts are reported in parts per million (δ) downfield from TMS, and coupling constants are reported in hertz (*Hz*). Proton coupling patterns are abbreviated as singlet (s), broad singlet (brs), doublet (d), triplet (t) and multiplet (m). Mass spectra were recorded on a Qstar (Applied Biosystem) ESI-MS mass spectrometer.

Scheme of synthesis and general procedure

After determining the antiproliferative effect of in the present study, ten sitosteryl esters (analogues of natural product sitosteryl oleate) were synthesised and screened for their antiproliferative activity in U87 MG cells. The synthesis of compounds 2a to 2j followed the general procedure outlined in Fig. 4. A solution of sitosterol in triethylamine was added to a solution of dichloromethane and different acid chlorides held at 0ºC. The resulting mixture was stirred for 72 h at room temperature. At the end of the reaction, it was filtered and washed with a saturated solution of sodium hydrogen carbonate, and finally with 5% HCl solution. The organic layer was dried over magnesium sulfate, filtered, and concentrated under reduced pressure. The compounds were purified by column chromatography and characterised by ^{1}H NMR, ^{13}C NMR, IR, and HRMS, as shown in Supplementary Table 2 and Supplementary Figs. S1-S12.

General procedure for the synthesis of compounds (2a-2j)

To a solution of dichloromethane (75 mL) and Acid chlorides (15 mmol) held at 0ºC, a solution of

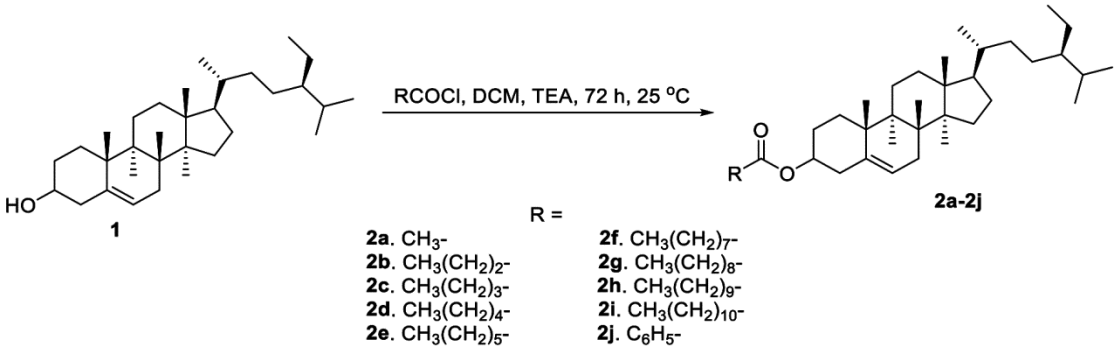

Fig. 4 — Synthesis of final compounds sitosteryl esters (2a-2j). Reagents and conditions: A) Acid chlorides, DCM, TEA, 72 h, 25°C.

sitosterol (4.14g, 10 mmol) in triethylamine (2 mL) was added. The resulting mixture was stirred for 72 hours at room temperature. At the end of the reaction, it was filtered and washed with a saturated solution of sodium hydrogen carbonate (100 mL) and finally with 5% HCl solution (100 mL). The organic layer was dried over magnesium sulfate, filtered, and concentrated under reduced pressure (25ºC, 15 mmHg). The white/off-white compounds obtained were further subjected to purification through column chromatography using ethyl acetate/cyclohexane (starting with 0.5% and increasing till 2.5%) as eluent to afford the pure compounds 2a-2j (overall yield 60-75%), and were further identified through HR-MS, IR, and NMR.

In-vitro studies

Cell cytotoxicity assay

U87 cells (1000 cells/well) and HEK (5000 cells/ well) were seeded into a 96-well plate and treated with sitosteryl analogues (described below) after 24 h at concentrations ranging from 5 μM to 200 μM. MTT assay was performed as mentioned previously in section 2.2.

Preparation of β-sitosteryl ester samples

Sitosteryl esters showed limited solubility in DMSO, which is the commonly used vehicle control. Therefore, we solubilised highly hydrophobic sitosteryl oleate derivatives in a Tween 20-water system. Briefly, sitosteryl esters (5 mg) were first dissolved in 1 mL of hexane to form the organic phase (dispersed phase). Before mixing with the aqueous phase, the organic phase was kept in a 50°C water bath for 5 min to facilitate dispersion of the sitosteryl ester. The aqueous phase (continuous phase) was prepared by dissolving Tween 20 at 2 g/L in Milli-Q water. The organic phase was slowly added to the aqueous phase under magnetic stirring (1000 rpm) and was immediately subjected to probe ultrasonic sonication for 10 min (pulse-on 3 s, pulse-off 3 s). Hexane was removed using a rotary evaporator attached to a circulating water bath under reduced pressure at 1 mbar. The cooling bath was set at 5°C.

Results

Characterisation of the bioactive compound isolated from the ether root extract (BDPT-3)

From spectroscopy, the structure of the compound isolated from the ether extract, sitosteryl oleate (BDPT-3), was determined. The spectroscopic data obtained were compared with those reported in the literature[49–51], and the compound was characterised as the oleic acid ester of sitosterol, i.e., sitosteryl oleate.

Sitosteryl oleate (1). Colourless liquid, $[\alpha]_D$ = -16 (c = 1 %, $CHCl_3$); IR: 1736.05 cm^{-1}; ^1H NMR (300 MHz, $CDCl_3$): δ 5.51-5.28 (m, 3 H), 4.52-4.07 (m, 1 H), 2.76-2.31 (m, 4 H), 2.08-1.81 (m, 9 H), 1.47-0.75 (m, 62 H), 0.68 (s, 3 H); ^{13}C NMR (300 MHz, $CDCl_3$): δ180, 140.65, 130.61, 130.16, 122, 74, 56.75, 56.05, 50.12, 45.83, 42.31, 39.77, 38.15, 37.23, 36.49, 36.13, 34.28, 33.94, 31.91, 31.85, 31.82, 29.75, 29.69, 29.65, 29.62, 29,51, 29.47, 29.35, 29.28, 28.86, 28.23, 27.21, 27.19, 26.08, 25.62, 24.80, 23.06, 22.68, 21.07, 19.80, 19.38, 19.02, 18.77, 14.10, 11.96, 11.84. ESI-MS m/z 679 (M^++1), 701 (M^++Na) calculated for $C_{47}H_{82}O_2$ (M^+) 678.^1H- and ^{13}C-NMR, and ^1H,^1H-COSY data shown in Supplementary Table 1.

Effects of sitosteryl oleate (BDPT-3) on cell proliferation

We studied the effects of sitosteryl oleate (BDPT-3) in various cancer cell lines. Typically, cells were treated with sitosteryl oleate (BDPT-3) (25-200 μg/mL) for 24 h, and the cell viability was assessed by trypan blue exclusion and MTT assay. The results showed that the BDPT3 caused cellular toxicity only in U87 cells. (Supplementary Fig. 13), whereas it was ineffective in HeLa, MCF7, MiaPaCa, and Colo205. The cell viability and proliferation decreased after treatment with increasing concentrations of sitosteryl oleate (BDPT-3) (Fig. 5). The IC_{50} value for the loss of metabolic viability was calculated to be 184 μM (125 μg/mL). When the cells were exposed to sitosteryl oleate (BDPT-3) at 200 μg/mL, cell proliferation was only 25% means and caused 75% cell death in U-87 cells. Similar results were

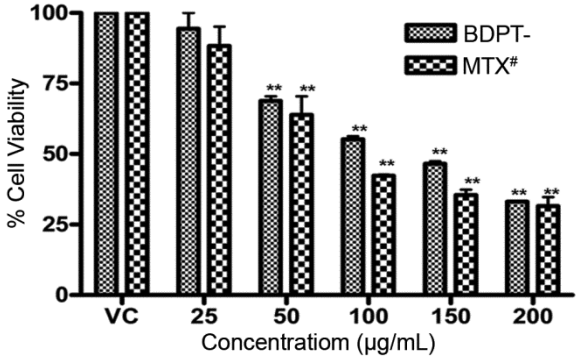

Fig. 5 — Effect of sitosteryl oleate (BDPT-3) on U-87 cells viability. Cultured cells were exposed to various concentrations of sitosteryl oleate (BDPT-3) for 24 h. Cell viability was analysed by MTT assay. #Methotrexate was at concentrations of 10, 20, 50, 100, and 200 nM. The result represents the average of three independent experiments in triplicate±S.D. **P <0.01.

obtained when we examined cytotoxicity using the trypan blue dye-exclusion method (Fig. 6), with the IC_{50} value of 169 µM (115 µg/mL). Detailed studies on the nature of toxicity were carried out at concentrations of 50 and 100 µg/mL corresponding to 40-50% cell death.

Effect on morphology

Changes in morphological features are suggestive of effects on cytoskeleton architecture, which is often associated with loss of viability and precedes death. Therefore, we examined morphological changes in U-87 cells using phase-contrast microscopy. Sitosteryl oleate (BDPT-3) induced morphological changes in U87, such as membrane blebbing, cell shrinkage, segregation of cellular structure, rounding, and detachment, which were evident at 24 h following exposure to 50 and 100 µg/mL of sitosteryl oleate (BDPT-3) (Fig. 7). These changes indicated that sitosteryl oleate (BDPT-3) might induce apoptotic cell death in U87 cells.

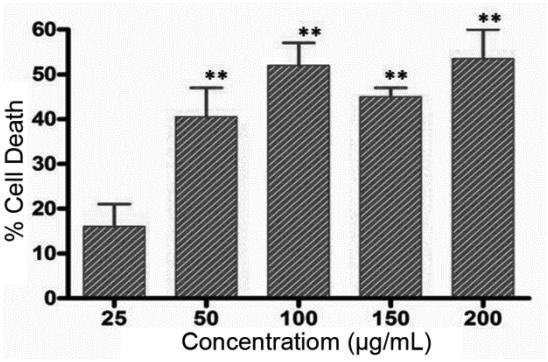

Fig. 6 — Effect of the sitosteryl oleate (BDPT-3) on the viability of U-87 cells checked by the trypan blue dye exclusion method. Cultured cells were exposed to various concentrations of sitosteryl oleate (BDPT-3) for 24 h. The result represents the average of three independent experiments in triplicate± S.D. **P <0.01.

Fluorescence microscopy: Acridine orange/Ethidium bromide (AO/EB) staining

Sitosteryl oleate (BDPT-3) treated U-87 cells were stained with AO/EB and analysed under a fluorescence microscope for the percentage of viable, apoptotic, and necrotic cells. The results obtained with AO/EB staining are represented in Fig. 8. Compared with the apoptosis observed in vehicle control cells (6.76±0.45%), U-87 cells treated with a low dose of sitosteryl oleate (BDPT-3) showed an increased percentage of apoptotic cells (50 µg/mL: 22.44±9%). A higher sitosteryl oleate (BDPT-3) dose, 100 µg/mL, significantly increased apoptosis in U-87 cells, with apoptotic cells predominating (62±10%). The percentage of necrotic cells remained approximately constant at a low level, independently of the sitosteryl oleate (BDPT-3) concentration. Fig. 8 shows the different morphologies of cells stained with AO/EB. The results suggest that sitosteryl oleate (BDPT-3) was able to induce marked apoptotic cellular death and, hence, characteristic morphological changes in U-87 cells.

Induction of DNA fragmentation

Since sitosteryl oleate (BDPT-3) induced morphological changes that suggest apoptotic death in U-87 cells, we studied the induction of internucleosomal fragmentation, an important hallmark of apoptosis. Incubation of cells with 50 and 100 µg/mL of sitosteryl oleate (BDPT-3) for 24 h significantly increased the DNA fragmentation (Fig. 9), whereas treatment with PEG: EtOH (2:3) (Negative control) did not produce any DNA fragmentation in U-87 cells under these conditions. Positive control-treated cells also showed DNA fragmentation.

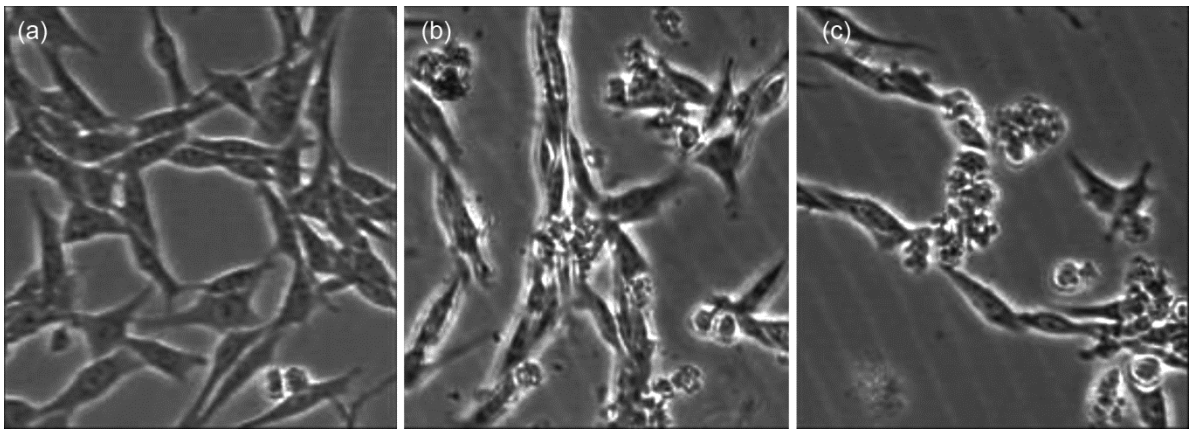

Fig. 7 — Effect of sitosteryl oleate (BDPT-3) on the morphology of the U-87 cells during 24 h of culturing, damage of the cytoplasmic membrane. (a) vehicle control cells, (b) concentration of 50 µg/mL, and (c) concentration of 100 µg/mL. Magnification of the microscope is 100X.

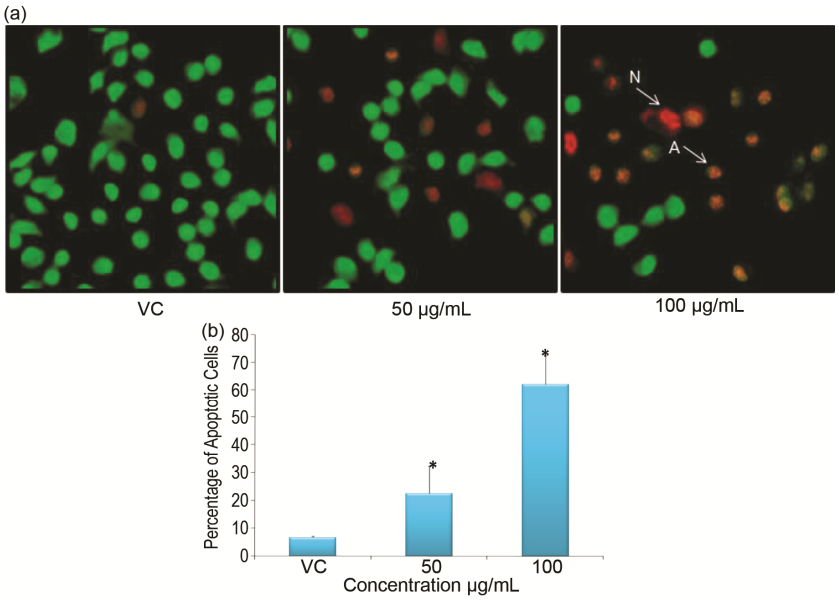

Fig. 8 — Percentage of apoptotic cell death measured by AO/EB staining. (a) Green viable cells with normal morphology were observed in the vehicle control (VC) group, orange apoptotic cells showed fragmented chromatin after 50 and 100 µg/mL sitosteryl oleate (BDPT-3) treatment for 24 h (marked by A) and red necrotic cells (marked by N). Magnification of microscope 100 X. (b) Graphical representation of percentage of apoptotic cells after treatment with sitosteryl oleate (BDPT-3).

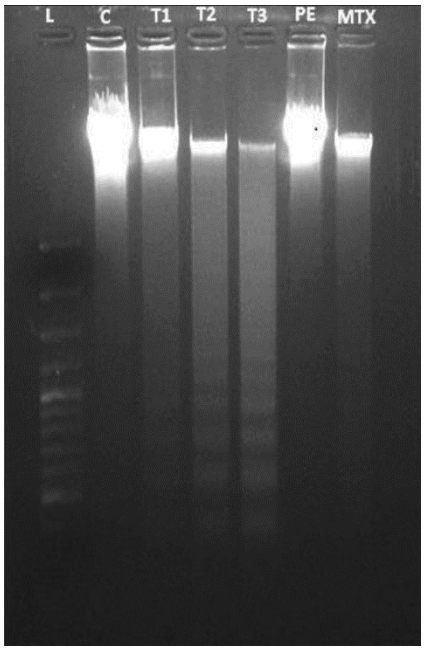

Fig. 9 — Sitosteryl oleate (BDPT-3) induced DNA fragmentation in U-87 cells. Genomic DNA was extracted from PEG: EtOH, sitosteryl oleate (BDPT-3), and Methotrexate treated U-87 cells after incubation for 24 h. Nucleosomal DNA fragments were resolved by electrophoresis in a 1.5% agarose gel and visualized by ethidium bromide staining. Lane 1 (L) - Ladder, Lane 2 (C) - Media control cells, Lane 3 (T1) – 50 µg/mL sitosteryl oleate (BDPT-3) treated cells, Lane 4 (T2)- 100 µg/mL sitosteryl oleate (BDPT-3) treated cells, Lane 5 (T3) – 200 µg/mL sitosteryl oleate (BDPT-3) treated cells, Lane 6 (PE) - PEG:EtOH (vehicle control) treated cells, Lane 7 (MTX) - Methotrexate (positive control) treated cells.

Sitosteryl Oleate (BDPT-3) caused apoptotic cell death without the cell cycle perturbations in U-87 cells

To determine whether the inhibition of sitosteryl oleate (BDPT-3) on U-87 cell-proliferation involved any cell cycle changes, we examined cell cycle phase distribution by DNA flow cytometry after 24 h of exposure to sitosteryl oleate (BDPT-3). Although significant alterations in the cell cycle distributions were not observed in sitosteryl oleate (BDPT-3) treated cells under these conditions, histograms clearly indicated the presence of degenerating cells, which is suggestive of apoptotic cells, in accordance with the observed DNA fragmentation. Quantitative analysis of the histograms showed a concentration-dependent increase in the hypodiploid region (sub-G1population) generally correlated with apoptotic cells, with more than 65% apoptosis at 200 µg/mL of sitosteryl oleate (BDPT-3) (Fig. 10) compared to the control.

Effects on Bax/Bcl-2 ratio

Levels of apoptotic and anti-apoptotic proteins following sitosteryl oleate (BDPT-3) treatment were examined by Western blots of the total protein to determine whether sitosteryl oleate (BDPT-3) induced apoptosis in U-87 by the intrinsic pathway, where the Bax/Bcl-2 ratio regulates cytochrome-c release, triggering the caspases. Treatment of U-87 cells with sitosteryl oleate (BDPT-3) did not cause significant changes in the expression of

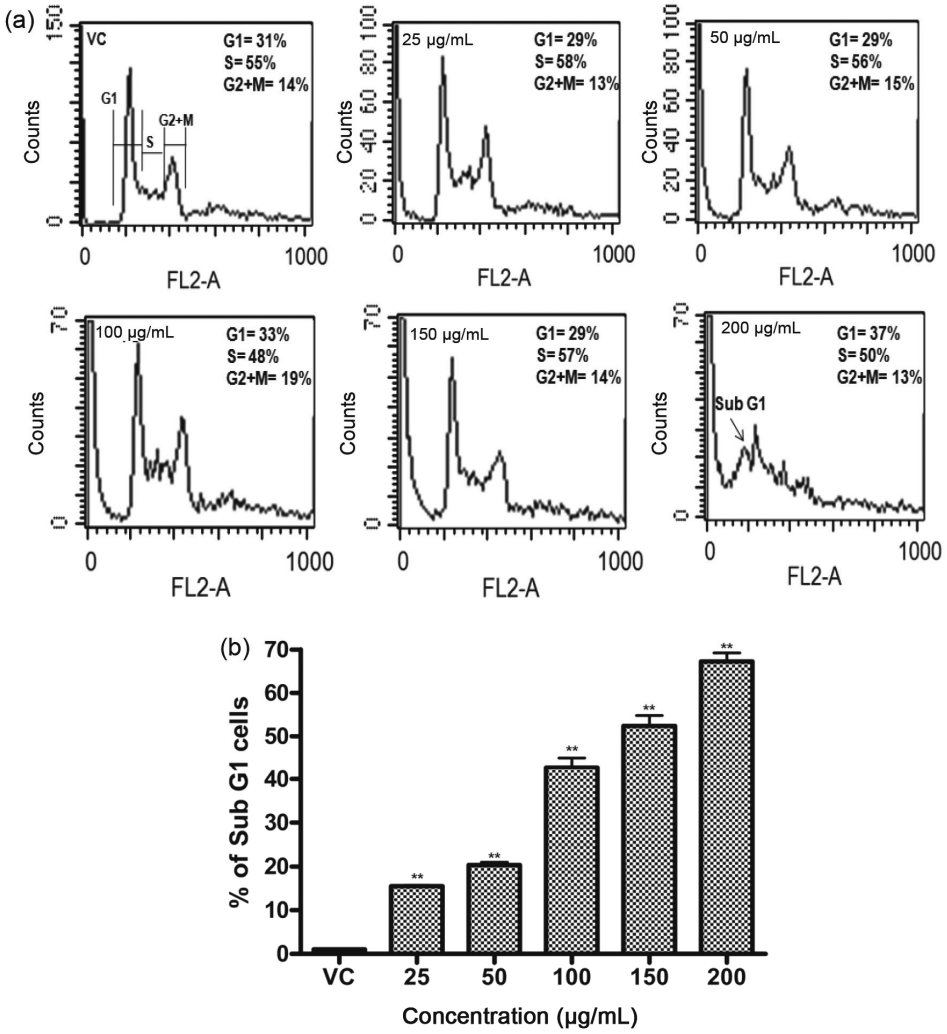

Fig. 10 — Sitosteryl oleate (BDPT-3) increases the apoptotic rates of cells. (a) After U-87 cells were grown in medium alone or treated with sitosteryl oleate (BDPT-3) in indicated concentrations, cells were harvested and washed with PBS, fixed with ice-cold 70% ethanol, stained with PI, and treated with RNase A. DNA content was measured by flow cytometry. The apoptotic population was measured as the percentage of the total cell population with <G1 DNA content. (b) Graphical representation of sub-G1 cells in vehicle control (VC) and sitosteryl oleate (BDPT-3) treated cells. The data are expressed as mean ± SE from three independent experiments. ** P <0.01.

Bax, while a significant decrease in the expression level of Bcl-2 was evident (Fig. 11a). A densitometric analysis of the bands showed that sitosteryl oleate (BDPT-3) resulted in a dose-dependent increase in the Bax/Bcl-2 ratio that favours apoptosis (Fig. 11b). Interestingly, there were no significant changes in the levels of p53 protein under these conditions (Fig. 11c).

Biological evaluation for analogues of β-sitosterol

In vitro antiproliferative activity

All the synthesised compounds were evaluated for their antiproliferative activity on U-87MG and HEK cells, and viability was examined at different concentrations of the synthesised compounds after 48 h using the MTT growth inhibition assay. Out of all the synthesised compounds, butanoate (2c), pentanoate (2d), and decanoate (2h) derivatives showed IC_{50} values between 60 and 70 µM, and benzoate (2j) showed an IC_{50} value of 91.77 µM after 72 h. All other compounds showed IC_{50} values above 100 µM. None of the compounds showed cytotoxicity on the normal cell line HEK up to a very high concentration (>250 µM). The results are shown in Table 1 and Fig. 12. The cytotoxic effects of all the compounds were calculated from a sigmoidal dose-response curve generated in GraphPad Prism 5.0.

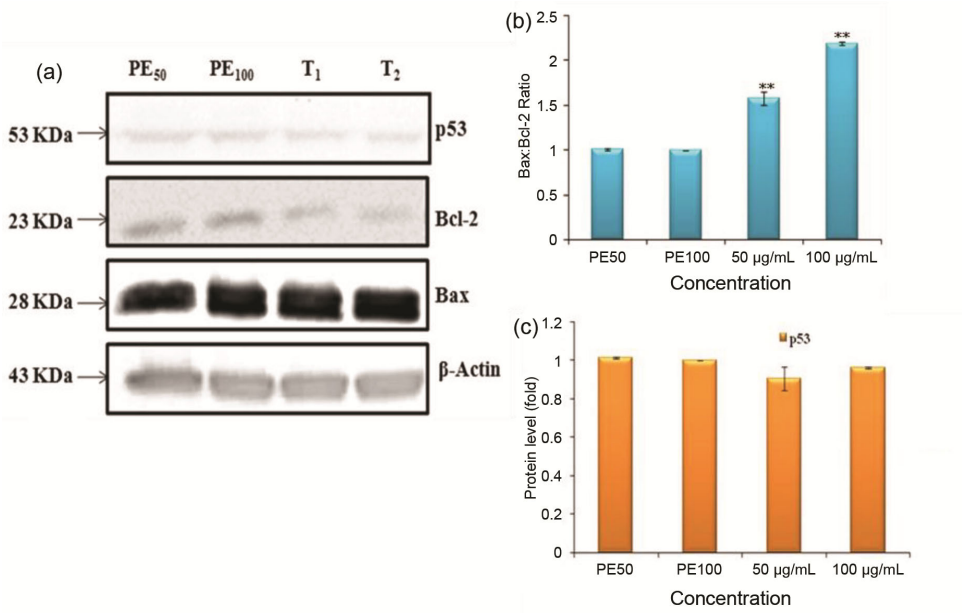

Fig. 11 — Immunoblot analysis of apoptosis-related protein expression in sitosteryl oleate (BDPT-3) treated U-87 cells. (a) Cells were lysed after 24 h of incubation with the indicated concentration of the sitosteryl oleate (BDPT-3). The cellular proteins were separated by SDS-PAGE and transferred onto PVDF membranes. The membranes were probed with the indicated primary antibodies, then with horseradish peroxidase-conjugated secondary antibody. β-Actin was used as an internal control. (b) Quantitative Bcl-2 and Bax expression after being standardized to β-Actin. The expression of Bcl-2 decreased, whereas the Bax protein level did not change after sitosteryl oleate (BDPT-3) treatment. (c) The integrated optical densities (IOD) of p53 protein after normalization with β-actin (43 kDa) in each lane using Gene Tools analysis software (Syngene). PE_{50} and PE_{100} were the vehicle controls for every 50 and 100 µg/ml treatment with sitosteryl oleate (BDPT-3), respectively. Paired values were evaluated by Student's t-test. (**P <0.01 compared with the control group).

Table 1 — *In vitro* antiproliferative activities of the synthesized sitosteryl ester derivatives (2a-2j) on U-87 MG cancerous cells and HEK normal cells after 72 h

Compounds	U87 (IC_{50}) μM	HEK (IC_{50}) μM	Selectivity Index IC_{50} (HEK)/ IC_{50} U87
2a (Acetate)	>100	>250	>2.5
2b (Propionate)	>100	>250	>2.5
2c (Butanoate)	70.32 ± 5.94	>250	>0.281
2d (Pentanoate)	69.38 ± 4.84	>250	>0.277
2e (Hexanoate)	>100	>250	>2.5
2f (Octanoate)	>100	>250	>2.5
2g (Nonanoate)	>100	>250	>2.5
2h (Decanoate)	64.89 ± 9.05	>250	>0.259
2i (Undecanoate)	>100	>250	>2.5
2j (Benzoate)	91.77 ± 9.17	>250	>0.367

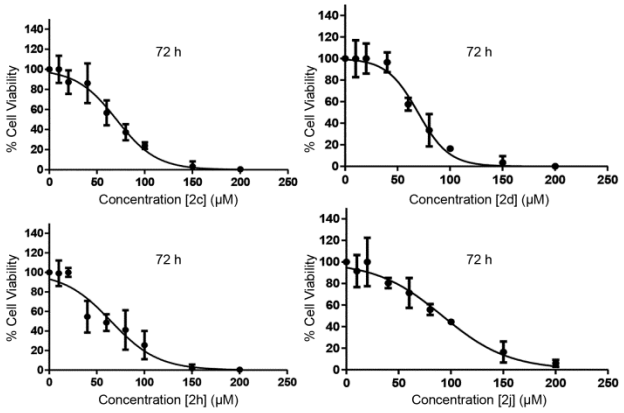

Fig. 12 — Effect of compounds 2c (butanoate), 2d (pentanoate), 2h (decanoate), and 2j(benzoate) on the viability of the U-87 cell line. Cytotoxicity effects of 2c, 2d, 2h and 2j evaluated after 72 h, calculated from sigmoidal dose response curves generated in Prism 5.0 (GraphPad) and expresses as % cell death.

Discussion

The plant-based diet can have protective action against cancer and other chronic diseases[52]. β-sitosterol, a plant compound known as a phytosterol and a counterpart of animal cholesterol, has several biological effects, such as anti-inflammatory, immune-modulating, and chemopreventive activities[53]. These effects strongly suggest that β–sitosterol might be an effective natural component in cancer chemoprevention. There are several ongoing research programs aimed at the isolation, structural characterisation, and pharmacological evaluation of bioactive plant secondary metabolites[54–56]. In this study, isolated compound sitosteryl oleate (BDPT-3) caused significant cell death in U-87MG cells. The structure of this compound was deduced by

comparing its spectroscopic data to that reported in the literature[57–60]. It was characterised as oleic acid ester of sitosterol, i.e., sitosteryl oleate (Supplementary Table 1). In the ^{1}H-NMR spectrum of sitosteryl oleate, the H-3 proton appeared as a multiplet at δ_H 4.15 (1H), and the H-6, H-9′, and H-10′ olefinic protons showed a multiplet at δ_H 5.36 (3H). There was a singlet at δ_H 0.68 (3H) and δ_H 0.98 (3H) for two methyl groups present at C-18 and C-19. The ^{13}C-NMR indicated the presence of a carbonyl (δ_C 180), suggesting that the isolated compound had an ester bond. Three ethylene carbons at δ_C 122 (C-6), δ_C 130.16 and 130.21 (C-9′ and C-10′) were also found. Positions 5 and 10 do not show any proton signal. We also found correlations in ^{1}H-^{1}H COSY spectra shown in Supplementary Table 1.

At the cellular level, some anticancer reagents provide partial remission by interfering with the processes of the cell cycle[61,62], while some others cause cell death by apoptosis[63], enhancing the probabilities of local tumour control. Dose-dependent cytotoxic effects of sitosteryl oleate (BDPT-3), as evidenced by many parameters investigated in the present study (Figs 5 and 6), suggest the therapeutic potential of sitosteryl oleate (BDPT-3). Although it induced both inhibition of proliferation and apoptosis of U-87 glioma cells in culture, it's *in vivo* efficacy needs to be examined before contemplating therapeutic application. Most cancer therapies aim to induce apoptosis in rapidly proliferating tumour cells. Therefore, drugs that can selectively target tumour cells with no harmful effects on normal ones are desired. Sitosteryl oleate (BDPT-3) causes visible morphological changes and DNA fragmentation in U-87 cells, which support the process of apoptosis induction by sitosteryl oleate (BDPT-3) (Figs. 7 and 8). After treatment with different concentrations of sitosteryl oleate (BDPT-3) for 24 h, the apoptotic cells increased significantly as shown by flow cytometry analyses (Fig. 10).

Regulatory proteins of the Bcl-2 family play an important role in the induction of apoptosis. The ratio of Bax to Bcl-2 determines, in part, the susceptibility of cells to death signals[64]. Therefore, Bcl-2 proteins have emerged as an attractive target for the development of novel anticancer drugs. Changes in the Bcl-2/Bax ratio have been reported to be caused by downregulation of Bcl-2 and upregulation of Bax[35], or downregulation of Bcl-2 with no change in the level of Bax[38]. Sitosterol oleate (BDPT-3) induced apoptotic cell death appears to involve the intrinsic pathway at least partly, as there was a significant increase in the Bax/Bcl-2 ratio (Fig. 11), which favours the release of cytochrome c from mitochondria into the cytoplasm, activating caspases involved in executing apoptosis. Our study parallels earlier observations, which demonstrated that β-sitosterol plays a role in triggering the intrinsic apoptosis pathway in a range of cancers, including multiple myeloma, lung cancer, melanoma, fibrosarcoma, pancreatic cancer, prostate cancer, liver cancer, cervical cancer, colon cancer, stomach cancer, breast cancer, leukaemia, and multiple myeloma[39]. Plant sterols, including β-sitosterol, have been shown in numerous studies to have antiproliferative effects on human breast cancer[28], liver cancer[34], colorectal cancer[33], and oral cancer[65]. However, further studies are required to understand the precise mechanism underlying sitosteryl oleate (BDPT-3) induced apoptosis, particularly identifying the primary signal (or events) responsible for the increase in Bax level.

DNA damage is known to increase the level and activation of the p53 tumour suppressor protein through damage-activated post-translational modifications, such as phosphorylation and acetylation. This results in transcriptional activation of the WAF1/CIP1/p21 gene, whose protein product triggers cell cycle arrest to permit DNA repair[66]. However, excessive damage or unsuccessful repair (leading to cumulative damage) triggers apoptosis to safeguard the genome[67]. P53 is known to regulate DNA repair, apoptosis, and cell cycle progression. However, not all forms of apoptosis and cell cycle arrest are p53-dependent[68,69]. Because more than half of human cancers have deficient p53[70], the p53-independent pathway has become a target for anticancer drugs[71]. Several studies to date have demonstrated that many natural phytochemicals can induce apoptosis and cell cycle arrest in p53- independent pathway[72,73]. Induction of apoptosis by sitosteryl oleate (BDPT-3) observed here appears to be p53 independent, as it did not cause any change in the level of p53.

In oral cancer (KB cells), cervical cancer (HeLa cells), *B. diffusa* root extracts were able to stimulate cell cycle arrest at various phases and enhance the percentage of cells in G0/G1-phase significantly, and the final results indicated that the extract could predominantly induce cell cycle arrest mainly in the DNA duplication phase[19,65]. In contrast, cells treated with *B. diffusa* extracts demonstrated G0-G1 arrest in

breast cancer (MCF-7 cells), enhancing the population of G0-G1 phase from 69.1% to 75.8% in comparison to the untreated control[74]. The flow cytometry revealed that sitosteryl oleate (BDPT-3) had no effect on the cell cycle profile of the U-87 MG cells, but apoptotic nuclei were identified in the hypodiploid region, which is the sub-G1 phase (Fig. 10).

The bioactivity-guided isolation and characterisation of sitosteryl oleate (BDPT-3) with its cytotoxic effects has been checked for the first time on U-87 myoglioma cells. Whereas, the antiproliferative activity of newly synthesised sitosteryl esters showed a lower IC_{50} in comparison to isolated sitosteryl oleate. Results concluded that the esters were successfully synthesised, as characterised by NMR, IR, and HRMS spectra. Sitosteryl butanoate (2c), sitosteryl pentanoate (2d), and sitosteryl decanoate (2h) showed an IC_{50} value of 60-70 µM on the U-87MG cell line, while the IC_{50} of these compounds was above 250 µM on HEK (normal cell line). The enhanced activity of these sitosteryl esters as compared to other derivatives suggests that esters with side-chain lengths of C-4, C-5, and C-10 show better activity. Therefore, the length and nature of side chains play a pivotal role in antiproliferative activity. This might be attributed to optimal lipophilicity, cellular uptake of short to medium length side chains, and enhanced cellular membrane interaction and retention of long side chains. These findings clearly demonstrate anticancer properties of these compounds in U87 cells and have future potential as an anticancer therapy for this highly malignant form of cancer.

Conclusion

The present study demonstrates the antiproliferative and apoptosis-inducing effects of sitosteryl oleate (BDPT-3) isolated from *B. diffusa in vitro*. Sitosteryl oleate induced a significant cytotoxic effect via dose-dependent inhibition of proliferation and induction of apoptosis, two important factors that enhance the efficacy of tumour therapy. Therefore, it appears that sitosteryl oleate isolated from *B. diffusa* is a potential anticancer agent that warrants further pre-clinical investigations in *in vivo* models. The designed derivatives of sitosteryl ester with shorter fatty acid chains were successfully synthesised in a one-step reaction and characterised by NMR (^{13}C and ^{1}H), IR, and HR-MS spectra. The characteristic ester peak was clearly observed in the IR spectra of the synthesised compounds at 1735 cm^{-1}, and these compounds showed antiproliferative activity against human glioma U87 cells. Butanoate (2c), pentanoate (2d), and decanoate (2h) esters showed an IC_{50} value between 60-70 µM on U87 MG cancerous cells.

One limitation of the study might be that the anticancer activity of the molecules was assessed using *in vitro* cell line-based assays. However, the study has translational potential, as the newly synthesised derivative can be further developed for *in vivo* and pre-clinical testing in appropriate tumour models. Therefore, the compounds in this work can be further evaluated preclinically in drug development procedures to create anticancer drugs that combat glioblastoma.

Conflicts of interest

The authors declare no conflict of interest.

Acknowledgement

Dr. R Srivastava is thankful to the Indian Council of Medical Research, New Delhi, for providing a Research Fellowship (DHR-Women Scientist Fellowship), 2018-2022. N Yadav is thankful to the Lady Tata Memorial Trust for providing a Research Fellowship, 2012-2017.

References

1 Sun W and Shahrajabian M H, Therapeutic potential of phenolic compounds in medicinal plants natural health products for human health, *Molecules*, 2023, **28**(4), 1845, doi: 10.3390/molecules28041845.

2 Adeola H A, Bano A, Vats R, Vashishtha A, Verma D, *et al.*, Bioactive compounds and their libraries: An insight into prospective phytotherapeutics approach for oral mucocutaneous cancers, *Biomed Pharmacother*, 2021, **141**, 111809, doi: 10.1016/j.biopha.2021.111809.

3 Tiwari P and Mishra K P, Role of plant-derived flavonoids in cancer treatment, *Nutr Cancer*, 2023, **75**(2), 430–449, doi: 10.1080/01635581.2022.2135744.

4 Hu H, Zhang S and Pan S, Characterization of citrus pectin oligosaccharides and their microbial metabolites as modulators of immunometabolism on macrophages, *J Agric Food Chem*, 2021, **69**(30), 8403–8414, doi: 10.1021/acs.jafc.1c01445.

5 Kitagawa T, Matsumoto T, Imahori D, Kobayashi M, Okayama M, *et al.*, Isolated from the *Fortunella crassifolia* and the citrus junos with their cell death-inducing activity on adriamycin-treated cancer cell, *J Nat Med*, 2021, **75**(4), 998–1004, doi: 10.1007/s11418-021-01528-8.

6 Cirmi S, Maugeri A, Lombardo G E, Russo C, Musumeci L, *et al.*, Flavonoid-rich extract of mandarin juice counteracts 6-OHDA-Induced oxidative stress in SH-SY5Y cells and modulates parkinson-related genes, *Antioxid Basel Switz*, 2021, **10**(4), 539, doi: 10.3390/antiox10040539.

7 Muhammad T, Ikram M, Ullah R, Rehman S U and Kim M O, Hesperetin, a citrus flavonoid, attenuates LPS-Induced neuroinflammation, apoptosis and memory

impairments by modulating TLR4/NF-κB signaling, *Nutrients*, 2019, **11**(3), 648, doi: 10.3390/nu11030648.

8 Dhuique-Mayer C, Gence L, Portet K, Tousch D and Poucheret P, Preventive action of retinoids in metabolic syndrome/type 2 diabetic rats fed with citrus functional food enriched in β-Cryptoxanthin, *Food Funct*, 2020, **11**(10), 9263–9271, doi: 10.1039/D0FO02430A.

9 Cataneo A H D, Kuczera D, Koishi A C, Zanluca C, Silveira G F, Arruda T B de, *et al.*, The citrus flavonoid naringenin impairs the *in vitro* infection of human cells by zika virus, *Sci Rep*, 2019, **9**(1), 16348, doi: 10.1038/s41598-019-52626-3.

10 Gansukh E, Nile A, Sivanesan I, Rengasamy K R R, Kim D H, *et al.*, Chemopreventive effect of β-Cryptoxanthin on human cervical carcinoma (HeLa) cells is modulated through oxidative stress-induced apoptosis, *Antioxid Basel Switz*, 2019, **9**(1), 28, doi: 10.3390/antiox9010028.

11 Song M, Lan Y, Wu X, Han Y, Wang M, *et al.*, The chemopreventive effect of 5-Demethylnobiletin, a unique citrus flavonoid, on colitis-driven colorectal carcinogenesis in mice is associated with its colonic metabolites, *Food Funct*, 2020, **11**(6), 4940–4952, doi: 10.1039/D0FO00616E.

12 Ahmed M B, Islam S U, Alghamdi A A A, Kamran M, Ahsan H, *et al.*, Phytochemicals as chemopreventive agents and signaling molecule modulators current role in cancer therapeutics and inflammation, *Int J Mol Sci*, 2022, **23**(24), 15765, doi: 10.3390/ijms232415765.

13 Gour R, *Boerhaavia diffusa* Linn plant a review one plant with many therapeutic uses, *Int J Pharm Sci Med*, 2021, **6**, 25–41, doi: 10.47760/ijpsm.2021.v06i04.003.

14 Nayak P and Thirunavoukkarasu M A, Review of the plant *Boerhaavia diffusa* its chemistry, pharmacology and therapeutical potential, *J Phytopharm*, 2016, **5**(2), 83–92, doi: 10.31254/phyto.2016.5208.

15 Dina J A, Nahar N, Sathi E T, Khatun M N and Jahan A, Evaluation of antioxidant, anticancer, anthelmintic, neuropharmacological activity of *Boerhaavia diffusa* Linn (Family Nyctaginaceae), *Eur J Med Plants*, 2024, **35**(6), 200–210, doi: 10.9734/ejmp/2024/v35i61219.

16 Gaur P K, Rastogi S and Lata K, Correlation between phytocompounds and pharmacological activities of *Boerhavia diffusa* Linn with traditional ethnopharmacological insights, *Phytomed Plus*, 2022, **2**(2), 100260, doi: 10.1016/j.phyplu.2022.100260.

17 Mehrotra S, Singh V K, Agarwal, S S, Maurya R and Srimal R C, Antilymphoproliferative activity of ethanolic extract of *Boerhaavia diffusa* roots, *Exp Mol Pathol*, 2002, **72**(3), 236–242, doi: 10.1006/exmp.2002.2427.

18 Hiruma Lima C A, Gracioso J S, Bighetti E J B, Germonsén Robineou L and Souza Brito A R M, The juice of fresh leaves of *Boerhaavia diffusa* L (Nyctaginaceae) markedly reduces pain in mice, *J Ethnopharmacol*, 2000, **71**(1), 267–274, doi: 10.1016/S0378-8741(00)00178-1.

19 Srivastava R, Saluja D, Dwarakanath B S and Chopra M, Inhibition of human cervical cancer cell growth by ethanolic extract of *Boerhaavia diffusa* Linn (Punarnava) root, *Evid Based Complement Alternat Med*, 2011, **2011**(1), 427031, doi: 10.1093/ecam/nep223.

20 Vikash A and Pankaj D, A review of the punarnawa (*Boerhaavia diffusa* linn) a plant with many medicinal uses, *Eur J Pharm Med Res*, 2023, **10**, 493.

21 Othman R A and Moghadasian M H, Beyond cholesterol-lowering effects of plant sterols: Clinical and experimental evidence of anti-inflammatory properties, *Nutr Rev*, 2011, **69**(7), 371–382, doi: 10.1111/j.1753-4887.2011.00399.x.

22 Moghadasian M H, Pharmacological properties of plant sterols *In vivo* and *in vitro* observations, *Life Sci*, 2000, **67**(6), 605–615, doi: 10.1016/S0024-3205(00)00665-2.

23 Smet E D, Mensink R P and Plat J, Effects of plant sterols and stanols on intestinal cholesterol metabolism suggested mechanisms from past to present, *Mol Nutr Food Res*, 2012, **56**(7), 1058–1072, doi: 10.1002/mnfr.201100722.

24 Li X, Xin Y, Mo Y, Marozik P, He T, *et al.*, The bioavailability and biological activities of phytosterols as modulators of cholesterol metabolism, *Molecules*, 2022, **27**(2), 523, doi: 10.3390/molecules27020523.

25 Makhmudova U, Schulze P C, Lütjohann D and Weingärtner O, Phytosterols and cardiovascular disease, *Curr Atheroscler Rep*, 2021, **23**(11), 68, doi: 10.1007/s11883-021-00964-x.

26 Turini E, Sarsale M, Petri D, Totaro M, Lucenteforte E, *et al.*, Efficacy of plant sterol-enriched food for primary prevention and treatment of hypercholesterolemia a systematic literature review, *Foods*, 2022, **11**(6), 839, doi: 10.3390/foods11060839.

27 Simonen P, Nylund L, Vartiainen E, Kovanen P T, Strandberg T E, *et al.*, Heart healthy diets including phytostanol ester consumption to reduce the risk of atherosclerotic cardiovascular diseases. a clinical review, *Lipids Health Dis*, 2024, **23**(1), 341, doi: 10.1186/s12944-024-02330-7.

28 Pradhan N, Parbin S, Kar S, Das L, Kirtana R, *et al.*, Epigenetic silencing of genes enhanced by collective role of reactive oxygen species and MAPK signaling downstream ERK/Snail axis ectopic application of hydrogen peroxide repress CDH1 gene by enhanced DNA methyltransferase activity in human breast cancer, *Biochim Biophys Acta BBA Mol Basis Dis*, 2019, **1865**(6), 1651–1665, doi: 10.1016/j.bbadis.2019.04.002.

29 Cheng D, Guo Z and Zhang S, Effect of β-Sitosterol on the expression of HPV E6 and P53 in cervical carcinoma cells, *Contemp Oncol*, 2015, **19**(1), 36, doi: 10.5114/wo.2015.50011.

30 Alvarez Sala A, Attanzio A, Tesoriere L, Garcia Llatas G, Barberá R, *et al.*, Apoptotic effect of a phytosterol-ingredient and its main phytosterol (β-Sitosterol) in human cancer cell lines, *Int J Food Sci Nutr*, 2019, **70**(3), 323–334, doi: 10.1080/09637486.2018.1511689.

31 Park Y J, Bang I J, Jeong M H, Kim H R, Lee D E, *et al.*, Effects of β-Sitosterol from corn silk on TGF-B1 induced epithelial mesenchymal transition in lung alveolar epithelial cells, *J Agric Food Chem*, 2019, **67**(35), 9789–9795, doi: 10.1021/acs.jafc.9b02730.

32 Shin E J, Choi H K, Sung M J, Park J H, Chung M Y, *et al.*, Anti-tumour effects of beta-sitosterol are mediated by AMPK/PTEN/HSP90 axis in AGS human gastric adenocarcinoma cells and xenograft mouse models, *Biochem Pharmacol*, 2018, **152**, 60–70, doi: 10.1016/j.bcp.2018.03.010.

33 Ma H, Yu Y, Wang M, Li Z, Xu H, *et al.*, Correlation between microbes and colorectal cancer tumor apoptosis is induced by sitosterols through promoting gut microbiota to

produce short-chain fatty acids, *Apoptosis*, 2019, **24**(1), 168–183, doi: 10.1007/s10495-018-1500-9.

34 Anwar M A, Tabassam, S, Gulfraz, M, Sheeraz Ahmad, M, Raja G K, *et al.*, Isolation of oxyberberine and β-Sitosterol from berberis lycium royle root bark extract and *in vitro* cytotoxicity against liver and lung cancer cell lines, *Evid Based Complement Alternat Med*, 2020, **2020**(1), 2596082, doi: 10.1155/2020/2596082.

35 Cao Z, Wang X, Lu L, Xu J, Li X, *et al.*, β-Sitosterol and gemcitabine exhibit synergistic anti pancreatic cancer activity by modulating apoptosis and inhibiting epithelial mesenchymal transition by deactivating Akt/GSK-3β signaling, *Front Pharmacol*, 2019, **9**, 1525, doi: 10.3389/fphar.2018.01525.

36 Sook S H, Lee H J, Kim J H, Sohn E J, Jung J H, *et al.*, Reactive oxygen species mediated activation of AMP activated protein kinase and c-Jun N-Terminal kinase plays a critical role in beta-sitosterol-induced apoptosis in multiple myeloma U266 cells, *Phytother Res PTR*, 2014, **28**(3), 387–394, doi: 10.1002/ptr.4999.

37 Bae H, Park S, Ham J, Song J, Hong T, *et al.*, Mitochondria calcium flux by β-Sitosterol promotes cell death in ovarian cancer, *Antioxidants*, 2021, **10**(10), 1583, doi: 10.3390/antiox10101583.

38 Pradhan N, Parbin S, Kausar C, Kar S, Mawatwal S, *et al.*, *Paederia foetida* induces anticancer activity by modulating chromatin modification enzymes and altering pro-inflammatory cytokine gene expression in human prostate cancer cells, *Food Chem Toxicol*, 2019, **130**, 161–173, doi: 10.1016/j.fct.2019.05.016.

39 Wang H, Wang Z, Zhang Z, Liu J and Hong L, β-Sitosterol as a promising anticancer agent for chemoprevention and chemotherapy mechanisms of action and future prospects, *Adv Nutr Bethesda Md*, 2023, **14**(5), 1085–1110, doi: 10.1016/j.advnut.2023.05.013.

40 Dolai N, Kumar A, Islam A and Haldar P K, Apoptogenic effects of β-Sitosterol glucoside from *castanopsis indica* leaves, *Nat Prod Res*, 2016, **30**(4), 482–485, doi: 10.1080/14786419.2015.1023201.

41 Raj R K D, β-Sitosterol-assisted silver nanoparticles activates Nrf2 and triggers mitochondrial apoptosis via oxidative stress in human hepatocellular cancer cell line, *J Biomed Mater Res A*, 2020, **108**(9), 1899–1908, doi: 10.1002/jbm.a.36953.

42 Aghaei Zarch S M, Nia A H, Nouri M, Mousavinasab F, Najafi S, *et al.*, The impact of particulate matters on apoptosis in various organs: mechanistic and therapeutic perspectives, *Biomed Pharmacother*, 2023, **165**, 115054, doi: 10.1016/j.biopha.2023.115054.

43 Elkoshi Z, Cancer and autoimmune diseases a tale of two immunological opposites, *Front Immunol*, 2022, **13**, doi: 10.3389/fimmu.2022.821598.

44 Molecular targeted therapy of glioblastoma Cancer Treatment Reviews https://www.cancertreatmentreviews.com/article/S0305-7372(19)30112-4/abstract (accessed 2025-01-06).

45 Barnholtz Sloan J S, Ostrom Q T and Cote D, Epidemiology of brain tumors, *Neurol Clin*, 2018, **36**(3), 395–419, doi: 10.1016/j.ncl.2018.04.001.

46 Davis M E, Glioblastoma overview of disease and treatment, *Clin J Oncol Nurs*, 2016, **20**(5 Suppl), S2-8, doi: 10.1188/16.CJON.S1.2-8.

47 Zhao M, van Straten D, Broekman M L D, Préat V and Schiffelers R M, Nanocarrier-based drug combination therapy for glioblastoma, *Theranostics*, 2020, **10**(3), 1355–1372, doi: 10.7150/thno.38147.

48 Zhang Q Y, Wang F X, Jia K K and Kong L D, Natural product interventions for chemotherapy and radiotherapy-induced side effects, *Front Pharmacol*, 2018, **9**, doi: 10.3389/fphar.2018.01253.

49 Cytotoxic Pentacyclic Triterpenoids from the Rhizome of Astilbe chinensis Sun 2003 Helvetica Chimica Acta Wiley Online Library, https://onlinelibrary.wiley.com/doi/abs/10.1002/hlca.200390194 (accessed 2025-01-17).

50 Julien David D, Geoffroy P, Marchioni E, Raul F, Aoudé Werner D, *et al.*, Synthesis of highly pure oxyphytosterols and (Oxy) phytosterol esters part II (Oxy)-Sitosterol esters derived from oleic acid and from 9,10-Dihydroxystearic acid, *Steroids*, 2008, **73**(11), 1098–1109, doi: 10.1016/j.steroids.2008.04.010.

51 Nguyen A T, Malonne H, Duez P, Vanhaelen Fastre R, Vanhaelen M, *et al.*, Cytotoxic constituents from *Plumbago Zeylanica*, *Fitoterapia*, 2004, **75**(5), 500–504, doi: 10.1016/j.fitote.2004.03.009.

52 Craig W J, Mangels A R, Fresán U, Marsh K, Miles F L, *et al.*, The safe and effective use of plant based diets with guidelines for health professionals, *Nutrients*, 2021, **13**(11), 4144, doi: 10.3390/nu13114144.

53 Khan Z, Nath N, Rauf A, Emran T B, Mitra S, *et al.*, Multifunctional roles and pharmacological potential of β-sitosterol emerging evidence toward clinical applications, *Chem Biol Interact*, 2022, **365**, 110117, doi: 10.1016/j.cbi.2022.110117.

54 Lim S M, Agatonovic Kustrin S, Lim F T and Ramasamy K, High performance thin layer chromatography based phytochemical and bioactivity characterisation of anticancer endophytic fungal extracts derived from marine plants, *J Pharm Biomed Anal*, 2021, **193**, 113702, doi: 10.1016/j.jpba.2020.113702.

55 El Zehery H R A, Ashry N M, Faiesal A A, Attia M S, Abdel-Maksoud M A, *et al.*, Antibacterial and anticancer potential of bioactive compounds and secondary metabolites of endophytic fungi isolated from *Anethum graveolens*, *Front Microbiol*, 2024, **15**, doi: 10.3389/fmicb.2024.1448191.

56 Ahmed S S T, Fahim J R, Youssif K A, AboulMagd A M, Amin M N, *et al.*, Metabolomics of the secondary metabolites of *Ammi visnaga* L roots (Family Apiaceae) and evaluation of their biological potential, *South Afr J Bot*, 2022, **149**, 860–869, doi: 10.1016/j.sajb.2022.01.011.

57 Dimethyl 9-Octadecenedioate and 9-Oktadecene from Methyl Oleate Via a Ruthenium-Catalyzed Homo Olefin Metathesis Reaction, ResearchGate, https://www.researchgate.net/publication/322081285_Dimethyl_9-Octadecenedioate_and_9-Oktadecene_from_Methyl_Oleate_Via_a_Ruthenium-Catalyzed_Homo_Olefin_Metathesis_Reaction (accessed 2024-11-19).

58 Synthesis of polyols containing nitrogen-phosphorus from vegetable oil derivatives for polyurethane film applications, https://www.researchgate.net/publication/351126843_Synthesis_of_polyols_containing_nitrogen-phosphorus_from_vegetable_oil_derivatives_for_polyurethane_film_applications?_tp=eyJjb250ZXh0Ijp7ImZpcnN0UG

FnZSI6Il9kaXJlY3QiLCJwYWdlIjoiX2RpcmVjdCJ9fQ (accessed 2024-11-19).

59 Isolation of phytoconstituents from the stems of *Mussaenda erythrophylla*, ResearchGate, https://www.researchgate.net/publication/225034218_Isolation_of_phytoconstituents_from_the_stems_of_Mussaenda_erythrophylla (accessed 2024-11-19).

60 Encapsulation of β-Sitosterol in Polyurethane by Sol–Gel Electrospinning. ResearchGate. https://www.researchgate.net/publication/311359928_Encapsulation_of_b-Sitosterol_in_Polyurethane_by_Sol-Gel_Electrospinning (accessed 2024-11-19).

61 Kaur S, Rajoria P and Chopra M, Ricolinostat suppresses proliferation, promotes apoptosis, and enhances the antiproliferative activity of topoisomerase inhibitors in cervical cancer cells, *Drug Dev Res*, 2022, **83**(8), 1822–1830, doi: 10.1002/ddr.21999.

62 El Dash Y, Elzayat E, Abdou A M and Hassan R, A novel thienopyrimidine-aminothiazole hybrids design, synthesis, antimicrobial screening, anticancer activity, effects on cell cycle profile, Caspase-3 mediated apoptosis and VEGFR-2 inhibition, *Bioorganic Chem*, 2021, **114**, 105137, doi: 10.1016/j.bioorg.2021.105137.

63 Jaskulska A, Janecka A E and Gach Janczak K, Thapsigargin from traditional medicine to anticancer drug, *Int J Mol Sci*, 2021, **22**(1), 4, doi: 10.3390/ijms22010004.

64 Alam M, Alam S, Shamsi A, Adnan M, Elasbali A M, *et al.*, M I, Bax/Bcl-2 Cascade Is Regulated by the EGFR pathway therapeutic targeting of non-small cell lung cancer, *Front Oncol*, 2022, **12**, doi: 10.3389/fonc.2022.869672.

65 Gunaseelan D, Ali M S, Albert A, Prabhakaran R, Beno D L, *et al.*, Biochemical and molecular anticancer approaches for *Boerhaavia diffusa* root extracts in oral cancer, *J Cancer Res Ther*, 2022, **18**(Suppl 2), S244, doi: 10.4103/jcrt.JCRT_932_20.

66 Pourrajab F, Zare Khormizi M R, Hekmatimoghaddam S and Hashemi A S, Molecular targeting and rational chemotherapy in acute myeloid leukemia, *J Exp Pharmacol*, 2020, **12**, 107–128, doi: 10.2147/JEP.S254334.

67 Huang R and Zhou P K, DNA damage repair: Historical perspectives, mechanistic pathways and clinical translation for targeted cancer therapy, *Signal Transduct Target Ther*, 2021, **6**(1), 1–35, doi: 10.1038/s41392-021-00648-7.

68 Kulaberoglu Y, Hergovich A, Gómez V, The Role of P53/P21/P16 in DNA Damage Signaling and DNA Repair, In *Genome Stability (Second Edition)*, vol 26, edited by I Kovalchuk, O Kovalchuk, (Translational Epigenetics, Academic Press, Boston), 2021, 257–274, doi: 10.1016/B978-0-323-85679-9.00015-5.

69 Feroz W and Sheikh A M A, Exploring the multiple roles of guardian of the genome P53, *Egypt J Med Hum Genet*, 2020, **21**(1), 49, doi: 10.1186/s43042-020-00089-x.

70 Marei H E, Althani A, Afifi N, Hasan A, Caceci T, *et al.*, P53 Signaling in cancer progression and therapy, *Cancer Cell Int*, 2021, **21**(1), 703, doi: 10.1186/s12935-021-02396-8.

71 Drugging p53 in cancer one protein, many targets, *Nat Rev Drug Discov*, https://www.nature.com/articles/s41573-022-00571-8 (accessed 2024-11-12).

72 Rahman N, Khan H, Zia A, Khan A, Fakhri S, *et al.*, Bcl-2 modulation in P53 signaling pathway by flavonoids A potential strategy towards the treatment of cancer, *Int J Mol Sci*, 2021, **22**(21), 11315, doi: 10.3390/ijms222111315.

73 Elsherbini A M, Sheweita S A and Sultan A S, Pterostilbene as a phytochemical compound induces signaling pathways involved in the apoptosis and death of mutant P53-Breast cancer cell lines, *Nutr Cancer*, 2021, **73**(10), 1976–1984, doi: 10.1080/01635581.2020.1817513.

74 Sreeja S and Sreeja S, An *in vitro* study on antiproliferative and antiestrogenic effects of *Boerhaavia diffusa* L extracts, *J Ethnopharmacol*, 2009, **126**(2), 221–225, doi: 10.1016/j.jep.2009.08.041.